FEMS Microbiology Ecology, 2022, **98**, 1–11
DOI: 10.1093/femsec/fiac132
Advance access publication date: 10 November 2022
Research Article

Seasonal dynamic of diazotrophic activity and environmental variables affecting it in the Gulf of Riga, Baltic Sea

Ineta Liepina-Leimane*, Ieva Barda, Iveta Jurgensone, Atis Labucis, Natalija Suhareva, Vendija Kozlova, Agita Maderniece, Juris Aigars

Latvian Institute of Aquatic Ecology, Agency of Daugavpils University, Voleru Street 4, Riga, Latvia, LV-1007
***Corresponding author:** Voleru street 4, Riga, Latvia, LV-1007. E-mail: ineta.liepina@lhei.lv
Editor: Martin W. Hahn

Abstract

The semi-enclosed Baltic Sea experiences regular summer blooms of diazotrophic cyanobacteria. Previously, it has been conclusively demonstrated that in open nitrogen-limited parts of the Baltic Sea, cyanobacteria successfully fix atmospheric N_2. At the same time, diazotrophic activity is still poorly understood in Baltic Sea sub-regions where nitrogen and phosphorus are co-limiting primary production. To address this gap in research, we used the ^{15} N tracer method for *in situ* incubations and measured the N_2-fixation rate of heterocyst-forming cyanobacteria and picocyanobacteria in the Gulf of Riga, Baltic Sea, from April to September. Physicochemical variables and phytoplankton community composition were also determined. Our results show that the dominant species of cyanobacteria for this region (*Aphanizomenon flosaquae*) was present in the phytoplankton community during most of the study period. We also establish that the N_2-fixation rate has a strong correlation with the proportion of *A. flosaquae* biomass containing heterocysts ($r = 0.80$). Our findings highlight the importance of a heterocyst-focused approach for an accurate diazotrophic activity evaluation that is one of the foundations for future management and protection of the Baltic Sea.

Keywords: *Aphanizomenon flosaquae*, Baltic Sea, diazotrophic cyanobacteria, heterocysts, N_2-fixation

Introduction

N_2-fixing or diazotrophic cyanobacteria are considered the gatekeepers of bioavailable nitrogen and primary productivity in the open ocean. The estimated marine diazotroph contribution on the global scale is from 90 Tg (Kolber 2006) to 130–280 Tg (Konno et al. 2010, Eugster and Gruber 2012) of fixed nitrogen annually. Diazotroph-derived nitrogen assimilation of the dissolved atmospheric N_2 in temperate and coastal marine systems is also considerable. Nitrogen fixation in the Baltic Sea alone supplies 0.03 to 0.434 Tg of nitrogen annually (Rahm et al. 2000, Larsson et al. 2001, Wasmund et al. 2001, 2005, Rolff et al. 2007).

The wide range of estimated atmospheric nitrogen deposition and its subsequent utilization by marine organisms in the Baltic Sea reflects a disparity of measured N_2-fixation rates that could be as low as 0.17 nmol-N h^{-1} L^{-1} (Eigemann et al. 2019) or as high as 41 nmol-N h^{-1} L^{-1} (Ploug et al. 2011). There is a common perception that the temporal and spatial variation of the N_2-fixation rate is regulated by environmental conditions such as the availability of inorganic phosphorus (i.e. low inorganic nitrogen to phosphorus ratio), light intensity, temperature, turbulence and water-column mixing depth (Howarth et al. 1988). Furthermore, the cyanobacteria blooms are heterogeneous between Baltic Sea sub-basins in regard to the N_2-fixing taxa. Throughout the region, three predominant diazotrophic cyanobacteria—*Nodularia spumigena*, *Aphanizomenon* and *Dolichospermum* (formerly *Anabaena*)—are found in various proportions (Niemi 1979, Wasmund 1997). This factor of diazotrophic cyanobacteria species composition has been addressed in several recent studies (Wasmund et al. 2001, Ploug et al. 2011, Klawonn et al. 2016, Eigemann et al. 2019) when estimating N_2-fixation rates.

The variation of N_2-fixation rate makes extrapolation of values measured in short-term summer cruises across all cyanobacteria productive season challenging. The attempts to use abundance (Degerholm et al. 2008) or biomass of filamentous cyanobacteria (Wasmund et al. 2001, Zilius et al. 2021) have been successful on some occasions. At the same time, the inability to estimate N_2-fixation from diazotrophic cyanobacteria biomass alone has also been stressed (Wasmund et al. 2001). Although Moisander et al. (1996) and Zilius et al. (2021) have demonstrated N_2-fixation rate dependence from the abundance of heterocysts—specialized cells for N_2-fixation—the work of Lindahl and Wallstrom (1985) has shown that their activity and therefore the N_2-fixation rate can vary. Furthermore, even although most common diazotrophic cyanobacteria found in the Baltic Sea form heterocysts, some unicellular picocyanobacteria (< 2 μm) have also been proposed to contribute to the fixed nitrogen (Wasmund et al. 2001).

There is a long history of N_2-fixation studies in the Baltic Sea. However, there have been only a few studies targeting the whole productive season of *Aphanizomenon* sp. that dominates the Baltic Sea central and coastal areas (Degerholm et al. 2008) and the highly productive Curonian Lagoon (Zilius et al. 2021). The attempts to estimate the contribution to N_2-fixation of non-heterocystous diazotrophs (i.e. picocyanobacteria) are even fewer (Wasmund et al. 2001). Therefore, in this study we aimed to in-

Received: April 29, 2022. **Revised:** October 30, 2022. **Accepted:** November 7, 2022

vestigate the seasonal pattern of heterocyst-forming cyanobacteria N_2-fixation rates as well as estimate N_2-fixation by picocyanobacteria in the coastal waters of the Gulf of Riga, Baltic Sea. We demonstrate that the parameters associated with diazotrophic activity are best explained by variables characterizing the *Aphanizomenon flosaquae* population and that the N_2-fixation rate is linked to the proportion of heterocysts containing biomass of *A. flosaquae*. We also provide empirical evidence that non-heterocystous picocyanobacteria cells are able to fix N_2.

Materials and Methods

Study area

The Gulf of Riga is a relatively shallow, semi-enclosed sub-basin of the Baltic Sea with an average depth of 26.2 m, water volume of 424 km^3 and water residence time of 2 to 4 years (Yurkovskis et al. 1999, Purina et al. 2018). It is strongly influenced by freshwater runoff, because its drainage area significantly exceeds the Gulf of Riga surface area.

The phytoplankton seasonal succession in the Gulf of Riga follows the general pattern for temperate coastal waters with a spring bloom of diatoms that, in a later period, are taken over by dinoflagellates and ciliates. Summer blooms are characterized by cyanobacteria often accompanied by chlorophytes and cryptophytes, and afterwards follows the second peak of diatoms in autumn (Yurkovskis et al. 1999, Jurgensone et al. 2011, Labucis et al. 2017, Purina et al. 2018, Tunēns et al. 2022).

For study purposes, a 20-m deep coastal station (Fig. 1) was chosen so that it is outside the direct influence of river discharge and represents coastal conditions.

Sampling

Seawater was collected with a Van Dorn water sampler 11 times during the period from April to September 2021 from the Latvian Institute of Aquatic Ecology Vessel "Ronis2" (see the sampling dates in Supplementary Table 1). Samples for nutrient concentration analysis were taken at depths of 0.5, 2.5 and 5 m, transferred to 1-liter plastic bottles and kept in the dark at 5°C until they were analyzed in the laboratory. Additionally, samples from depths of 0.5, 2.5 and 5 m were taken for chlorophyll *a* (Chl *a*) analysis, and phytoplankton community as well as picoplankton biomass determination. The samples for Chl *a* analysis were filtered on glass fiber filters (Whatmann GF/F), placed in the exicator and kept in the freezer until further treatment. The samples (300 ml) for phytoplankton community analyses were fixed with Lugol's solution, acidic (final conc. 0.5%) immediately after sampling and stored in the dark until further analyses in the laboratory. Picoplankton samples (50 ml) were fixed with glutaraldehyde (final conc. 1%) immediately after sampling and stored in the dark until further analyses in the laboratory.

Profiles of water temperature and salinity were measured using a CTD probe (SBE 19plus Sea-Cat, Sea-Bird Scientific, USA) with a vertical resolution of 0.5 m. Profile of photosynthetically active radiation (PAR, 0-10 m) was measured with a LI-COR Data Logger and LI-190R Quantum Sensor. Turbidity (0-10 m) was profiled with a digital water quality meter (YSI ProDSS). These measurements of vertical profiles were repeated each hour throughout the incubation period to acquire average diurnal values. The real-time measurement database of the Skulte Port smart buoy situated 2 km from the sampling station was used to determine the current speed during the sampling occasions.

Analytical procedures

The concentration of Chl *a* was measured according to HELCOM Monitoring Guidelines (HELCOM 2017). Chl *a* was extracted from a glass fiber filter in 96% ethanol for 24 h and analyzed using a spectrophotometer (Cary 100 Conc UV–Visible Spectrophotometer). Oxygen concentrations were determined with a sensor before and after incubation (PreSens Fibox 4) and converted to carbon units according to the stoichiometry of the photosynthesis equation. Net primary production (NPP, gC $m^{-2}d^{-1}$) was calculated by subtracting initial oxygen concentrations from the final oxygen concentrations at each sampling depth: 0.5, 2.5 and 5 m.

Nutrient concentrations were determined according to Grasshoff et al. (1999). The inorganic dissolved phosphate (DIP) and ammonium (NH_4^+) concentrations were measured using the molybdenum blue and indophenol blue methods, respectively. Nitrite (NO_2^-) and nitrate (NO_3), after reduction to nitrite in a copper-coated cadmium column, were determined by nitrite reaction with an azo dye. Dissolved inorganic nitrogen (DIN) was expressed as the sum of ammonium, nitrite and nitrate.

Microscopy

For phytoplankton community determination, subsamples of 10 ml were analyzed using an inverted microscope. Individual cells were counted according to HELCOM Monitoring Guidelines (HELCOM 2021). Subsamples were settled in a sedimentation chamber for 12 h and counted at 200x and 400x magnification (Uthermöl 1958). The number of counted cells in all subsamples exceeded 500. The wet weight of the phytoplankton biomass was expressed as mg m^{-3} and calculated in accordance with Olenina et al. (2006). Phytoplankton organisms were identified to the lowest possible rank. Scientific names and classification were compiled with the accepted binomial nomenclature of the World Register of Marine Species (version 2021).

For picoplankton analyses, subsamples of 5 ml were filtered with <10 kPa vacuum onto an Irgalan black-stained 0.2-μm pore-sized Nuclepore polycarbonate filter and stained with proflavine (Hobbie et al. 1977). The filter was mounted on paraffin oil and picocyanobacteria cells were counted with an epifluorescence microscope at 100x oil immersion objective under green excitation light. At least 50 cells were counted on each filter. The volume of picocyanobacteria was expressed as the average of 50 individual cell measurements and the cell shape dimensions were used to calculate wet weight (mg m^{-3}, Edler 1979).

Incubations with $^{15}N_2$-enriched water

The collected seawater at 0.5, 2.5 and 5 m was prepared for two parallel series of incubation for each depth to acquire the total N_2-fixation rate and the picocyanobacteria N_2-fixation rate. For the total N_2-fixation rate, seawater was transferred to 500-ml Duran glass bottles directly without any pre-treatment. For the picocyanobacteria N_2-fixation rate, the collected seawater was filtered through a 10-μm mesh stainless steel sieve (Humboldt, No. 850, frame diameter 25.4 cm) before being transferred to 500-ml Duran glass bottles. To ensure that filaments and individual cells of cyanobacteria were removed by filtration, samples from the filtered bulk volume were investigated using an inverted microscope. Both non-filtered and filtered sample series for each depth consisted of three replicate bottles. Thereafter, the bottles were sealed with bromobutyl rubber stoppers and 50 ml of the seawater was replaced with 50 ml of MiliQ water enriched with $^{15}N_2$ through an injection. The enriched MiliQ water used to spike incubation bottles was pre-prepared based on adjusted methodological rec-

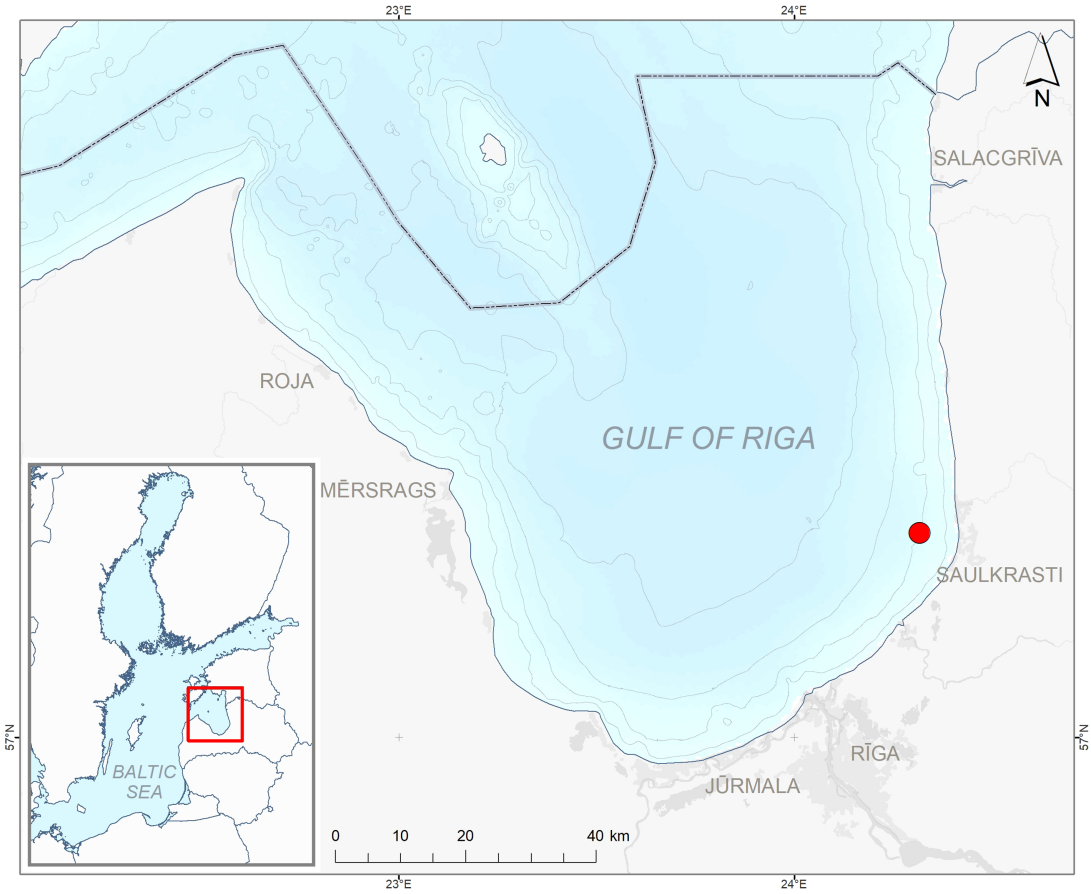

Figure 1. Sampling and incubation site.

ommendations by Klawonn et al. (2015). For each sampling occasion, 900 ml of degassed MiliQ water (sonicated for 1 h, 60°C) was transferred to a Tedlar gas sampling bag (push lock valve, 1 L) and spiked with 9 ml of $^{15}N_2$ gas (Sigma-Aldrich, 98 atom% ^{15} N). The filled gas sampling bag was left for 24 h at 8°C before being used to dissolve the $^{15}N_2$ gas bubble in the MiliQ water. After enriching the seawater, the bottles were placed and secured in a stainless-steel frame that was deployed to the corresponding depth the sample was taken from. The samples were then incubated for 10–12 h corresponding to the diurnal time of the day. The ^{15} N atom% in the enriched samples was expressed as the sum of added and naturally abundant ^{15} N. First, the total of dissolved N_2 in the sample was calculated based on the seawater temperature, salinity and N_2 solubility coefficients (A_0, A_1, A_2, A_3, B_0, B_1 and B_2) provided by Hamme and Emerson (2004):

$$lnC = A_0 + A_1 T_S + A_2 T_S^2 + A_3 T_S^3 + S\left(B_0 + B_1 T_S + B_2 T_S^2\right)$$

where C is the N_2 concentration at equilibrium with the atmosphere, T is the temperature (°C) and S is the salinity. After that, the natural nitrogen ratio in the atmosphere (^{15} N/^{14} N = 0.366 atom%) was used to determine the ^{15} N content in the sample. As a last step, the N_2 solubility formula was used to calculate ^{15} N in the 50 ml of enriched water assumed to contain only $^{15}N_2$ because the water was degassed prior to enrichment and added to the ^{15} N content in the sample. However, it must be acknowledged that a theoretical estimation of $^{15}N_2$ gas dissolution can result in some underestimation of rates (White et al. 2020).

After incubation, an aliquot subsample (50–100 ml) from each bottle and of the bulk volume used to fill incubation bottles was filtered on a pre-combusted (500°C for 2 h) 13-mm diameter GF/F filter for isotopic signature analysis with an elemental analyser (EuroEA-3024, EuroVector S.p.A, Italy) coupled with a continuous flow stable isotope ratio mass spectrometer (Nu-HORIZON, Nu Instruments Ltd, UK). The isotope ratio mass spectrometry analysis was performed in the Laboratory of Analytical Chemistry, University of Latvia. Isotope ratios were reported relative to atmospheric nitrogen for δ^{15}N as parts per thousands (‰):

$$\delta^{15}N = \left(\frac{(^{15}N/^{14}N)_{sample}}{(^{15}N/^{14}N)_{atmosphere}} - 1\right) \times 1000$$

where (^{15} N/^{14} N) $_{atmosphere}$ = 0.003676. To use a mass balance approach and determine the N_2-fixation rate as described by Montoya et al. (1996), the average of the three replicate δ^{15}N values was then converted to the absolute abundance ratio A (^{15} N atom%) of the ^{15} N enrichment of particulate N as follows:

$$A = 100 \times \frac{(10^{-3}\delta^{15}N + 1)(^{15}N/^{14}N)_{atmosphere}}{1 + (10^{-3}\delta^{15}N + 1)(^{15}N/^{14}N)_{atmosphere}}$$

The remainder of incubated seawater in the Duran bottles was used to filter a second batch of aliquot subsamples on pre-combusted (at 500°C for 2 h) 24-mm diameter GF/F filters for N% analysis (Elementar Vario El III). In addition, 0.4–1.4 L aliquot of bulk volume used to fill incubation bottles was filtered on pre-weighted nitrocellulose membrane (Millipore, 45-mm diameter, 0.45-μm pore size) to determine suspended particulate matter

(SPM). After drying (24 h, room temperature), the nitrocellulose filters were weighed again and SPM (mg L^{-1}) was calculated as follows:

$$SPM = \frac{m_{f+SPM} - m_f}{V}$$

where m_{f+SPM} is the mass of filter and SPM, m_f is the filter mass and V is the volume of bulk seawater filtered through the nitrocellulose filter.

Diurnal N_2-fixation rate (NFR, nmol N L^{-1}) was then estimated using the following equation (Montoya et al. 1996):

$$NFR = \frac{A_{PN} - A_{PN(0)}}{A_{N_2} - A_{PN(0)}} \times PN$$

where $A_{PN(0)}$ is the ^{15} N enrichment of particulate N before the incubation, A_{PN} is the ^{15} N enrichment of particulate N after the incubation and A_{N2} is the sum of naturally abundant and added ^{15} N. PN represents particulate nitrogen concentration at the end of the incubation period calculated based on the corresponding samples N% and SPM (transformed in nmol N L^{-1}). The heterocyst-forming cyanobacteria N_2-fixation rate was achieved by subtracting the picocyanobacteria N_2-fixation rate of pre-filtered seawater samples (<10 μm) from the total N_2-fixation rate. Because picocyanobacteria isotope signatures for week 32 and week 36 were not analyzed, the heterocyst-forming cyanobacteria N_2-fixation rate for these sampling occasions was obtained by subtracting the mean value of picocyanobacteria N_2-fixation rate throughout the whole sampling period (0.5 m = 3.2 nmol N L^{-1}, 2.5 m = 2.2 nmol N L^{-1}, 5 m = 0 nmol N L^{-1}) from the total rate.

Statistical analysis

R software v. 3.6.1 (R Core Team 2019) was used for data visualization and analysis of the environmental variables collected during the sampling period. An overview of the relationship between environmental variables was provided based on Spearman's rank correlation with the coefficient significance set at $\alpha = 0.05$. For multivariate analysis, the dependent matrix of parameters associated with diazotrophic activity (N_2-fixation rate, heterocyst abundance, proportion of *A. flosaquae* biomass containing heterocysts) was Hellinger-transformed. Detrended correspondence analysis was used to identify the appropriate response model for the dependent matrix of parameters associated with diazotrophic activity. Because the gradient length for all calculated axes was below 2, redundancy analysis (RDA) was applied. The explanatory variables or terms of both abiotic (PAR, DIN, DIP, NH_4^+, turbidity, current speed) and biotic (*A. flosaquae* total biomass and filament length) drivers were included in a global model. To construct a simplified model, automatic forward selection was applied to the RDA global model by retaining variables that significantly increased the adjusted R^2. The significance for the models, axis and terms was measured by a permutation test (n = 1000). The observations of the last sampling occasion (week 45) were not included in the RDA due to a lack of N_2-fixation rate measurements.

Results

Physicochemical variables

The temperature and nutrient concentrations (Supplementary Table 1) generally followed the seasonal pattern for the Gulf of Riga. The water temperature reached the suggested limit (8–10°C; Laamanen and Kuosa 2005, Mehnert et al. 2010) for filamentous cyanobacteria growth on 16 May (week 19). The water temperature indicated a stratification in the depth of up to 5 m from May (week 19) to July (week 28). Starting at the end of July (week 29) and until the last N_2-fixation rate measurements in September (week 38), there was no temperature gradient observed in the 0–5 mwater layer.

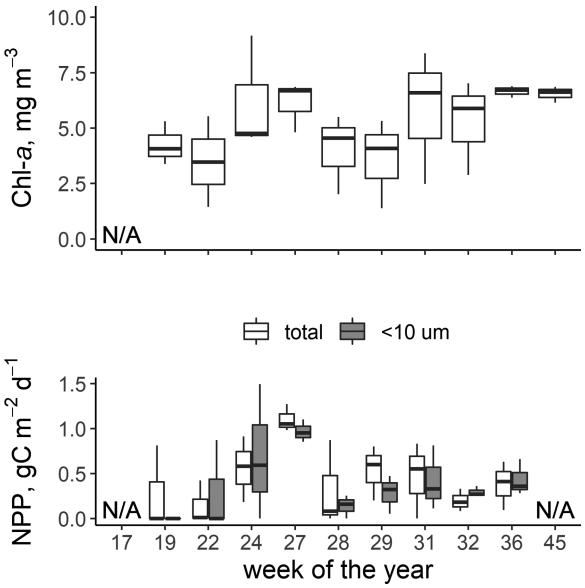

Figure 2. Seasonal dynamic of chlorophyll *a* and net primary production (NPP).

The concentrations of DIP varied from below the detection limit (<0.04 μmol L^{-1}) to 0.69 μmol L^{-1} and DIN varied from 0.14 μmol L^{-1} to 33.43 μmol L^{-1}. As expected, concentrations of both DIP and DIN were relatively low throughout the productive season (i.e. from May to September), except for on 17 June (week 24), when the highest concentrations of DIN and elevated concentrations of DIP were observed. Overall, the DIN: DIP ratio in the surface water layer (0–5 m) corresponded to the phosphorus-limited marine system, except for on 4 August (week 31) and on 11 September (week 36). However, at the sampling events during August and September, the observed DIN concentration was very low (<1 μmol L^{-1}), indicating possible DIN and DIP co-limitation.

Phytoplankton community dynamics

The NPP fluctuated in combination with Chl *a* concentrations (Fig. 2). An increase in both Chl *a* and NPP values was observed in late June to early July (weeks 24 to 27). A noticeable increase of Chl *a* was also observed in August–September (weeks 31 to 36); however, no corresponding increase in NPP was observed during those sampling events.

Cyanobacteria cells were present throughout the entire study period, although in April (week 17) their proportion of the total phytoplankton community was practically negligible (Fig. 3). Starting from May (week 19), the proportion of cyanobacteria started to increase, reaching a maxima of the total in June (0.5 and 2.5 m, week 24), July (5 m, week 28) and September (0.5, 2.5 and 5 m, week 36). On average, 90% of the cyanobacteria were nitrogen-fixing species, except for in September (week 36), when half of the counted cyanobacteria cells were representing nitrogen non-fixing cyanobacteria species. Overall, eight nitrogen-fixing taxons were identified (Supplementary Table 2). The most dominant (>90%) was *A. flosaquae*, with the exception of July (5 m,

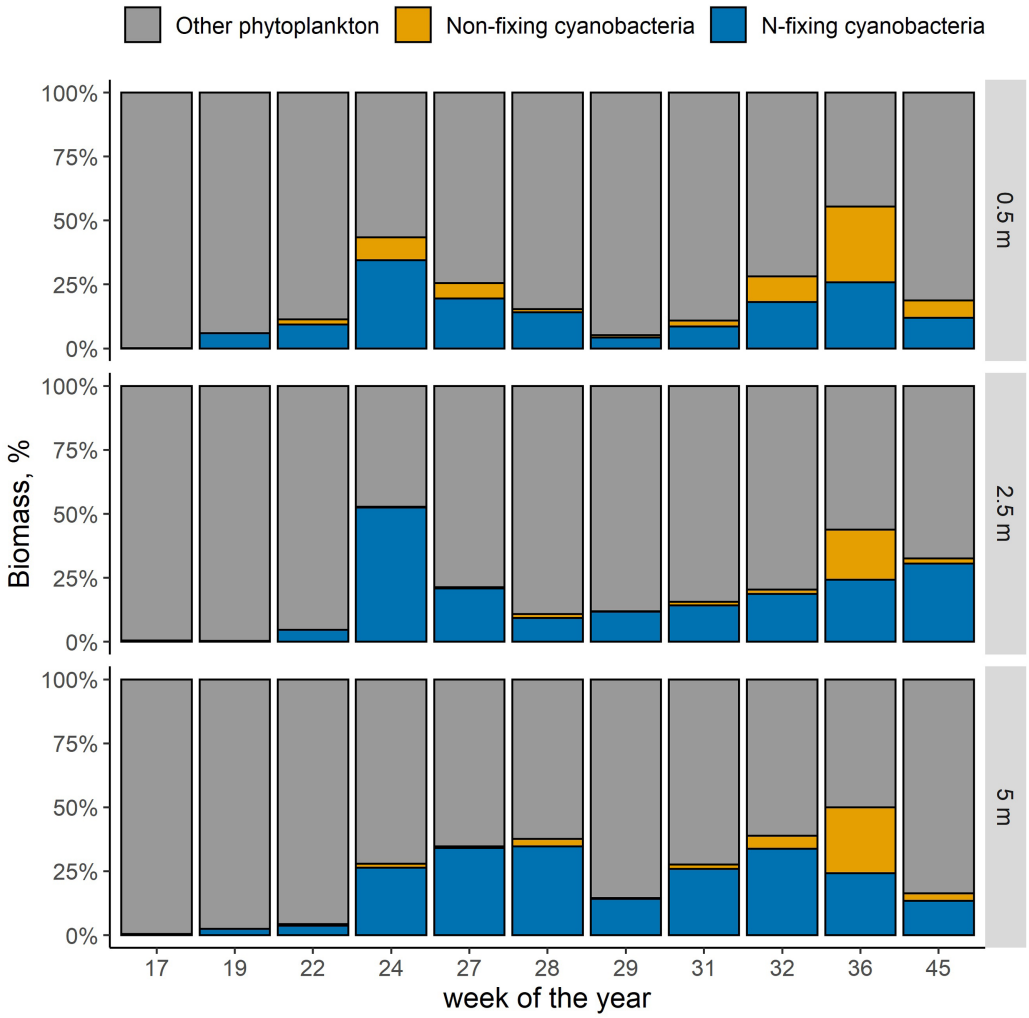

Figure 3. Proportion of N_2-fixing and non-fixing cyanobacteria at depths of 0.5, 2.5 and 5 m.

week 29) and August (0.5 and 5 m, week 31), when 19%–21% of cyanobacteria were *N. spumigena* filaments.

The cyanobacteria *A. flosaquae* started to develop heterocysts (Fig. 4) in two upper horizons (0.5 and 2.5 m) as early as in May (week 19). During the following months, the proportion of filaments that formed heterocysts increased, forming an intermediate maximum in June (week 22), until it peaked (44%) in the upper horizons during mid-August (week 32).

In the 5 m horizon, *A. flosaquae* started to develop heterocysts later than in the two uppermost ones. Furthermore, also the highest proportion (22%) of filaments containing heterocysts in the 5 m horizon was recorded later, in September (week 36), than in the two uppermost horizons. Overall, it should be stressed that throughout the study period, biomass of *A. flosaquae* without heterocysts was predominant.

Seasonal variation of N_2-fixation and heterocyst abundance

During the experiment, the heterocyst formation by *A. flosaquae* accompanied by N_2-fixation was detected (Fig. 5) as early as May (week 19). However, the observed N_2-fixation rate was very low (0–1.2 nmol N L^{-1}) and remained so until mid-July (week 28), except for on 17 June (week 24), when a noticeable increase in the N_2-fixation rate was observed in the 0.5 m horizon. The gradual increase of N_2-fixation rates started in late July (week 29) and reached the highest rate (0.5 m, 36.9 nmol N L^{-1}) in August (week 32). Thereafter, a decline in N_2-fixation rates was observed, although it should be noted that the N_2-fixation rates observed in September were substantially higher than those recorded during June–July. The average total N_2-fixation rates (Supplementary Table 2) generally follow the same pattern as was observed for the number of heterocysts (Fig. 5). The peak N_2-fixation rate, however, does not coincide with maximum heterocyst abundance, with the latter offset to September (week 36). Similarly, a considerable increase in the number of heterocysts was observed on 17 June (week 24) at the 2.5- and 5-m horizons that did not result in an increase in the N_2-fixation rates.

Incubation experiments with pre-filtered seawater samples (<10 μm) of N_2-fixation by picoplankton were performed from late April to early September. Due to equipment failure, the samples taken during weeks 32 and 36 were not analyzed and only results from late April to early August are used for the purposes of this study. During this period, the N_2-fixation rates (Fig. 6) were sporadic. Measurable values were only detected in May, June and from the end of July to August at the depths of 0.5 and 2.5 m. N_2-fixation rate values were in the range of 30%–33% of corresponding unfractionated samples, except for the 0.5-m layer in early August (week 31), which reached 42%. The observed steady increase in picocyanobacterial biomass from week 17 to week 32

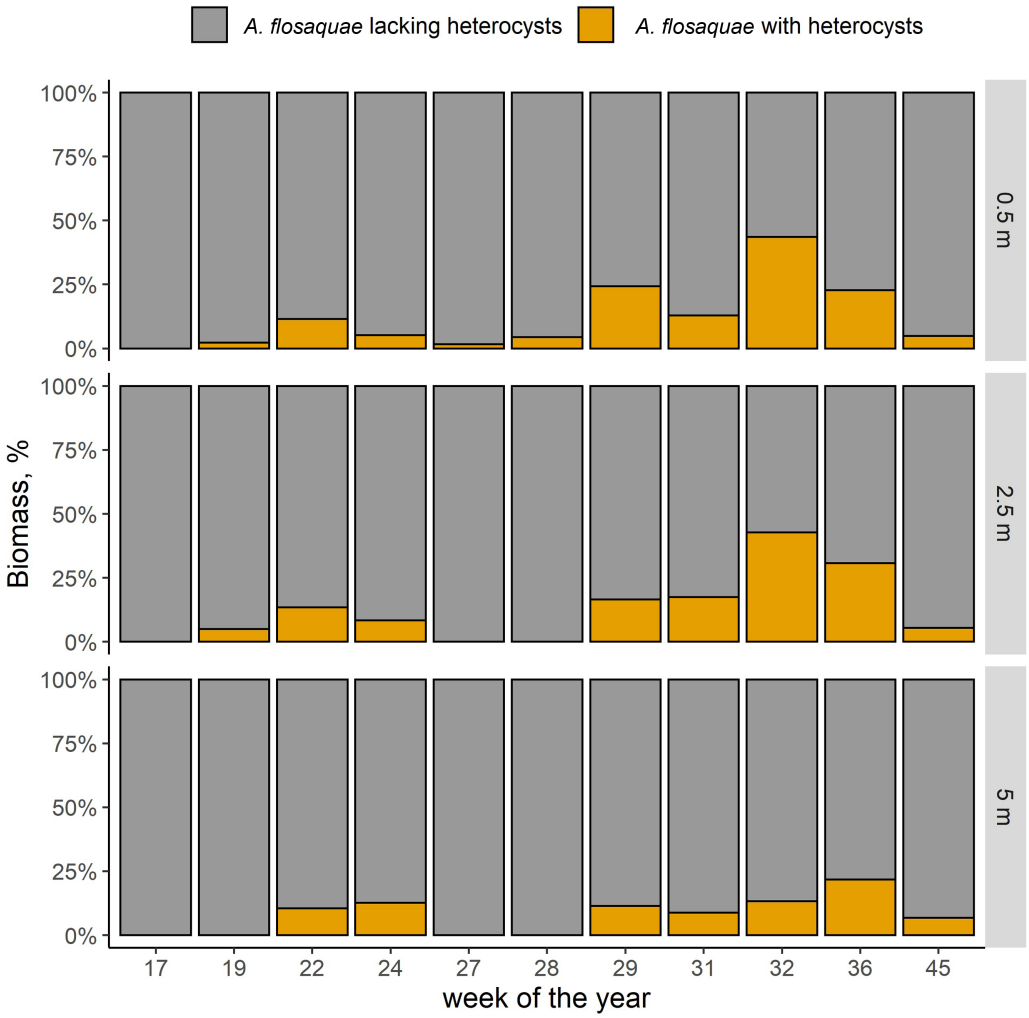

Figure 4. Proportion of *A. flosaquae* biomass containing heterocysts at depths of 0.5, 2.5 and 5 m.

did not, however, result in a corresponding increase in N_2-fixation rates. Due to the small size and lack of distinctive morphological features, microscopic examination yielded only picocyanobacterial biomass (Fig. 6). However, because the N_2-fixation rate was detected on only a few sampling occasions, it was not used as a variable for correlation purposes.

Relationships between diazotrophic activity and environmental variables

RDA was applied to reveal the canonical relationship between environmental variables and the parameters associated with diazotrophic activity, that is, the N_2-fixation rate, heterocyst abundance and the proportion of *A. flosaquae* biomass containing heterocysts. The environmental variables included in the global RDA model ($P \geq 0.001$) explain 67.8% of the variation of the parameters associated with diazotrophic activity from April to September when N_2-fixation was measured (Fig. 7A). Based on a permutation test of the global model, the first two canonical axes resulting from the RDA as well as five variables—current speed, DIP, PAR, total *A. flosaquae* biomass and filament length—are statistically significant ($P \leq 0.05$). After removing redundant environmental variables from the global model, only two—total *A. flosaquae* biomass and filament length—were selected for a simplified RDA model (Fig. 7B). The simplified model explains 67.4% of the variation of the parameters associated with diazotrophic activity. The permutation test indicates that the simplified model and the first two of its canonical axes are significant ($P \geq 0.001$).

In addition to the RDA, environmental variables measured at depths of 0.5, 2.5 and 5 m are presented in a Spearman's rank correlation coefficient matrix (Fig. 8). Several positive statistically significant and strong correlations for the N_2-fixation rate and associated parameters are displayed, such as with heterocyst abundance, heterocyst containing *A. flosaquae* biomass and filament length. However, the strongest correlator for N_2-fixation rate was the proportion of *A. flosaquae* heterocyst containing biomass (Fig. 8).

Our results demonstrate a complex relationship between *A. flosaquae* biomass and heterocyst development. Generally, an increase in total *A. flosaquae* biomass is expected to indicate a higher biomass of *A. flosaquae* containing heterocysts. However, the portion of the heterocyst containing biomass does not correlate with the total *A. flosaquae* biomass. On the other hand, heterocyst proportion does correlate strongly with the filament and heterocyst length.

Only two physicochemical variables demonstrated a notable impact on the N_2-fixation rate or associated biological parameters. We established a positive correlation between the current speed and the *A. flosaquae* biomass containing heterocysts, the proportion of *A. flosaquae* heterocyst containing biomass, hetero-

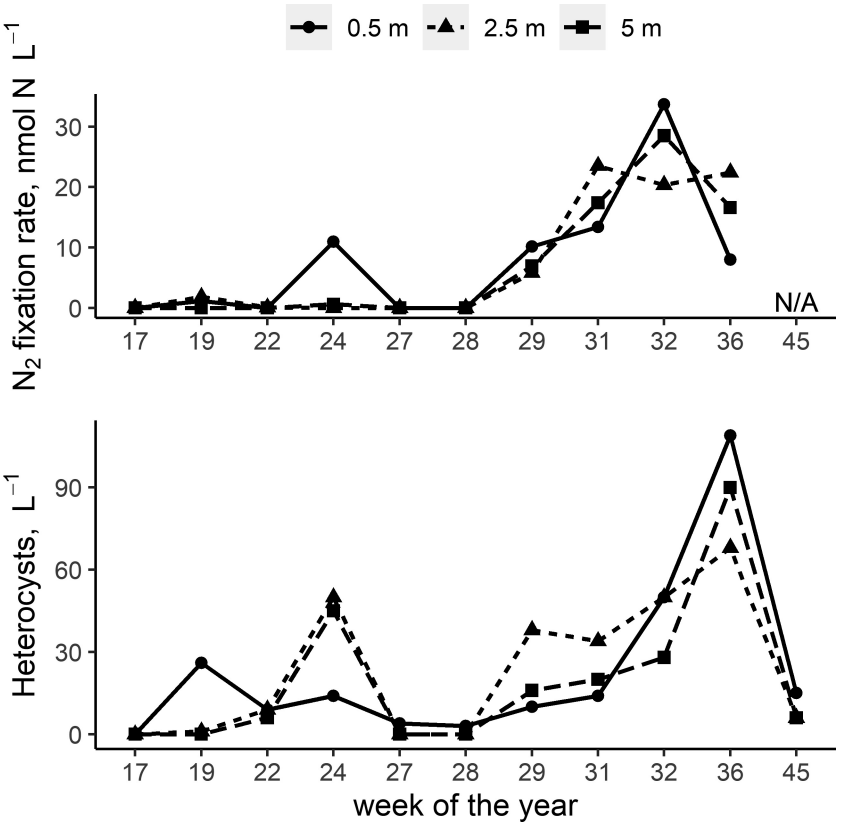

Figure 5. Heterocyst-forming cyanobacteria N_2-fixation rate seasonal dynamic and the corresponding heterocyst abundance in *A. flosaquae*.

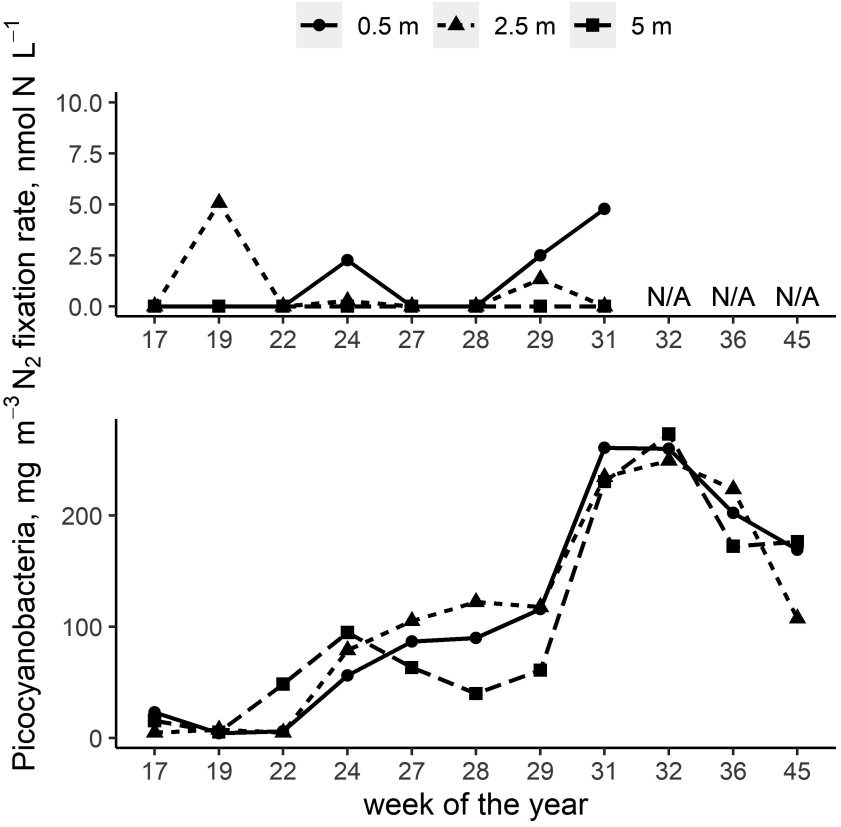

Figure 6. Seasonal dynamic of N_2-fixation rate and biomass of picocyanobacteria.

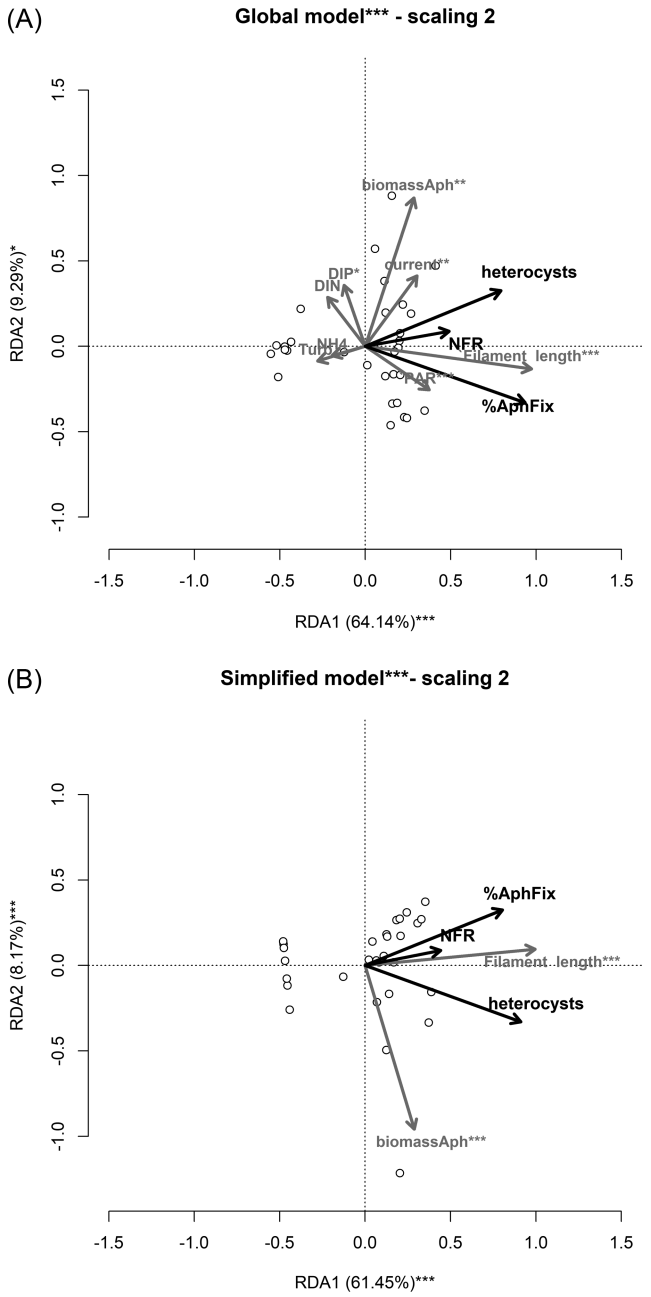

Figure 7. Ordination diagram based on RDA between diazotrophic activity parameters (NFR = N_2-fixation rate, heterocysts = heterocyst abundance, %AphFix = proportion of *A. flosaquae* biomass containing heterocysts). **(A)** A global model of all environmental variables (current = current speed, turb. = turbidity, biomassAph = total *A. flosaquae* biomass). **(B)** Simplified model containing environmental variables obtained after forward stepwise selection. Significant environmental variables and RDA axes are labeled accordingly: ***–0.001≥ *P*; **–0.001< *P* ≤0.01; *–0.01< *P* ≤0.05.

cyst abundance and N_2-fixation rate. By contrast, the correlation between ammonia concentration and N_2-fixation rate was negative. Additionally, PAR had a weak positive correlation with filament and heterocyst length.

Discussion

The N_2-fixation rates observed in the coastal waters of the Gulf of Riga during this study are in the range of those reported for

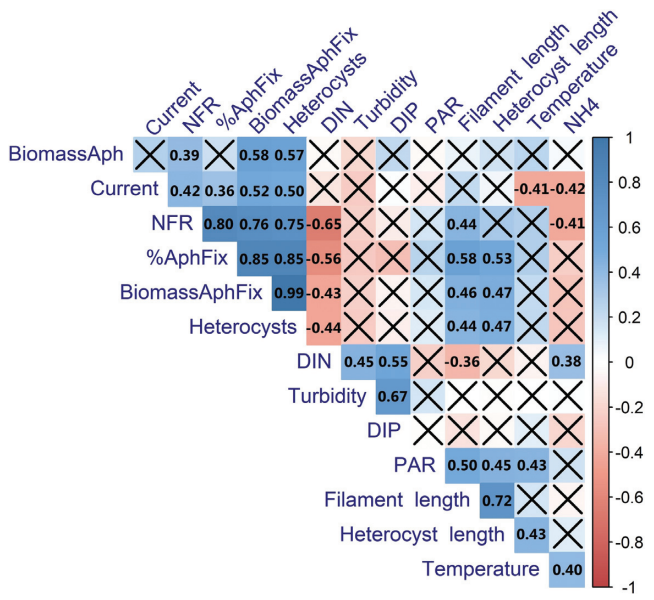

Figure 8. Spearman's rank correlation matrix containing statistically significant coefficients (NFR = N_2-fixation rate, heterocysts = heterocyst abundance, biomassAph = total *A. flosaquae* biomass, biomassAphFix = biomass of *A. flosaquae* containing heterocysts, %AphFix = proportion of *A. flosaquae* biomass containing heterocysts, current = current speed, NH4 = ammonium).

the Baltic Sea in the last two decades (Table 1). The findings of Eigemann et al. (2019) also support the empirical evidence provided herein that non-heterocystous diazotrophs contribute to N_2-fixation. However, an earlier overview of N_2-fixation rates summarized by Wasmund et al. (2001) displays more conservative N_2-fixation rates 40–50 years ago.

A number of previous studies have also addressed a variety of physicochemical and biological variables that potentially regulate the N_2-fixation rate. Most of those earlier studies were conducted in late summer–early autumn when the temperature is not considered to limit N_2-fixation. However, in studies covering the whole productive season, such as this study, the temperature could be an important abiotic driver for N_2-fixation, as suggested by Laamanen and Kuosa (2005). The results herein confirm the previously established cyanobacteria ability to form heterocysts and perform N_2-fixation at temperatures below 10°C (Zakrisson and Larsson 2014, Sveden et al. 2015). At the same time, similar to the conclusion made by Stal and Walsby (2000), the light availability expressed as PAR (Fig. 7A) seems to be more important than temperature. The impact of PAR on N_2-fixation, however, is mostly indirect as PAR correlates with filament length (Fig. 8), which is one of two main factors affecting N_2-fixation (Fig. 7B).

The role of the DIN: DIP ratio in triggering heterocyst formation in diazotrophic cyanobacteria and consequently governing N_2-fixation in the Baltic Sea is still uncertain. Although it has been suggested that a low DIN: DIP ratio might give a competitive advantage to N_2-fixing cyanobacteria (Smith 1983, Laamanen and Kuosa 2005), some later studies have argued that nitrogen depletion (Zakrisson and Larsson 2014) or availability (Vintila and El-Shehawy 2007) does not affect the N_2-fixation rate. Furthermore, it has been proposed that rather than the DIN: DIP ratio, the DIP availability is the factor affecting the growth of diazotrophic cyanobacteria and N_2-fixation (Olofsson et al. 2016). In this study we did not find an increase of N_2-fixation under low DIN: DIP conditions or during periods of elevated DIP concentrations. The Gulf

Table 1. Overview of reported N_2-fixation rates in the Baltic Sea.

Sub-basin	N_2-fixation rate	Heterocyst-forming species	Sampling period	Reference
Eastern Gotland Sea	Min: 0.21 nmol N L^{-1} h^{-1} Max: 23.6 nmol N L^{-1} h^{-1}	*Aphanizomenon* sp., except in August (*Nodularia* sp. 38.5%)	May–November 1997	Wasmund et al. (2001)
	0.05–5.52 nmol N L^{-1} h^{-1}	*Aphanizomenon* sp., except in July–August (*Nodularia* sp. 39.1%–61.5%)	February– November 1998	
Stockholm archipelago	26.7 ng N L^{-1} h^{-1} (1.91 nmol N L^{-1} h^{-1})	*Aphanizomenon* sp. (98%)	August 2000	Degerholm et al. 2008
Offshore, Baltic Proper	125.5 ng N L^{-1} h^{-1} (8.95 nmol N L^{-1} h^{-1})	*Aphanizomenon* sp. (95%)		
Stockholm archipelago	15 nmol N L^{-1} h^{-1}	*Aphanizomenon* sp.	August 2008	Ploug et al. 2010
Stockholm archipelago	41 nmol N L^{-1} h^{-1}	*Aphanizomenon* sp., *Anabaena* sp., *Nodularia* sp.	August 2009	Ploug et al. 2011
Stockholm archipelago	1.45 μmol N L^{-1} d^{-1} (1 m); 0.05 μmol N L^{-1} d^{-1} (12 m)	50% *Aphanizomenon* sp., 32% *Dolichospermum* sp., 18% *Nodularia* sp.	June–August 2012	Klawonn et al. 2016
Offshore, Baltic Proper	0.05 μmol N L^{-1} d^{-1} (1 m), 0.01μmol N L^{-1} d^{-1} (12 m)	50% *Aphanizomenon* sp., 36% *Dolichospermum* sp., 14% *Nodularia* sp.	June–August 2013	
Baltic Proper	0.17–1.03 nmol N L^{-1} h^{-1} 0.18–8.07 nmol N L^{-1} h^{-1}	*Aphanizomenon* sp. *Nodularia* sp.	August 2015	Eigemann et al. 2019
Curonian Lagoon	3.0 -4.6 μmol N L^{-1} d^{-1} (northern site); <0.4 μmol N L^{-1} d^{-1} (central site)	*Dolichospermum* sp., *Aphanizomenon* sp.	August–September 2018	Zilius et al. 2021
Danish Strait	0.7- 6 nmol N L^{-1} d^{-1}	dominated by *Nodularia*	September 2019	Reeder et al. 2021
Gulf of Riga	Diurnal: 0.1- 36.9 nmol N L^{-1}	*A. flosaquae* (>90%)	April–September 2021	This study

of Riga, especially its coastal areas, is a relatively shallow and dynamic water body periodically experiencing an influx of DIN and DIP enriched near-bottom water in the photic zone. Although it was expected that these events would affect the N_2-fixing capacity of diazotrophic cyanobacteria, our results indicate the opposite, because the highest N_2-fixation rates were observed during periods when the concentrations of both DIP and DIN were low. The low concentrations of DIP during periods of high N_2-fixation rates is most likely not the prerequisite, but rather a consequence, as cyanobacteria is incorporating DIP into biomass while assimilating N_2, thus depleting DIP from water media. Furthermore, because the biomass of *A. flosaquae* containing heterocysts did not exceed 50% on any of the sampling occasions, it can be concluded that a substantial fraction of the predominant species was not fixing N_2 but instead using DIN as an N source.

Even although physicochemical conditions could not be directly linked to the N_2-fixation rate, they remain important environmental drivers to look into as they likely affect biological variables that were directly linked to N_2-fixation rates. Previous studies have also addressed biological variables such as abundance or biomass of cyanobacteria (Wasmund et al. 2001, Degerholm et al. 2008) and abundance of heterocysts (Moisander et al. 1996, Zilius et al. 2021). Zilius et al. (2021) were even able to demonstrate a consistent relationship between biomass of phytoplankton, expressed as chlorophyll *a*, and N_2-fixation rate, because the phytoplankton biomass increase over the summer season was primarily driven by an increase in biomass of N_2-fixing species. By contrast, in this study, only on one sampling occasion did N_2-fixing species exceed 50% of the total biomass of phytoplankton. Consequently, there was no correlation between N_2-fixation rate and the total biomass of phytoplankton. Furthermore, even correlation between total biomass of the most abundant N_2-fixing species *A. flosaquae* and N_2-fixation rate was relatively weak. At the same time, a significant strong positive correlation of heterocyst abundance, and by association biomass of *A. flosaquae* filaments that contains heterocysts, with N_2-fixation rate, corresponded to previous findings by Moisander et al. (1996) and Zilius et al. (2021). The consistently low *A. flosaquae* filament biomass that developed heterocysts as well as the high variability of proportion of *A. flosaquae* biomass containing heterocysts, is most likely the reason why in this study no profound correlation between the total *A. flosaquae* biomass and N_2-fixation rate was established.

Although the correlation between heterocysts and N_2-fixation rate emphasizes the crucial role of heterocysts in N_2-fixation in the Gulf of Riga, the relationship is substantially weaker than in previous reports (Findlay et al. 1994, Zilius et al. 2021). This suggests that a simple abundance of heterocysts is not the most accurate indicator of the actual N_2-fixation rate in the Gulf of Riga because their activity varies, as previously reported by Lindahl and Wallstrom (1985).

The heterocyst formation is a terminal and a relatively fast process (Kumar et al. 2010), which for *Aphanizomenon* sp. is not characterized by a developmental pattern along the filaments like for the *Dolichospermum* sp. and *Nodularia* sp. (Yoon and Golden 2001; Voss et al. 2013). It could be argued that there are short-term or localized physicochemical conditions that trigger the formation of heterocysts in a small proportion of the *A. flosaquae* population. Thereafter, the conditions shift and heterocysts become redundant and less active. However, if environmental conditions that promote the formation of heterocysts persist for a longer period, a larger proportion of the diazotrophically active *A. flosaquae* population is able to form. As our results show, the proportion of *A. flosaquae* biomass containing heterocysts is a more precise proxy of the N_2-fixation rate than heterocyst abundance in ecosystems that are not N-limited.

This assumption at the present stage is still speculative, however, it does explain some of the differences when comparing N_2-fixation rates between aquatic systems. In the Curonian Lagoon

(Zilius et al. 2021), the excess DIP throughout the summer season facilitates *A. flosaquae* cell growth depending on the available P supply (Degerholm et al. 2006, Chen et al. 2020), while in the Gulf of Riga nutrient conditions change relatively fast and seem to limit the development of the *A. flosaquae* population. Similar findings have been reported in a study of Clear Lake, North America, that concluded that the annual N_2-fixation is best described by the proportion of heterocysts to vegetative cells in *A. flosaquae* (Horne and Goldman 1972).

Conclusions

This study illustrates that the diazotrophic activity in the Gulf of Riga has a seasonal pattern that broadly corresponds to the heterocyst abundance in *A. flosaquae* filaments and that the N_2-fixation rate reaches its peak during the cyanobacteria summer bloom. We were also able to confirm that picocyanobacteria are capable of fixing N_2 at a rate comparable with that exhibited by heterocysts-forming species, but it is overall limited to the surface water layer. The data acquired in this study, however, do not indicate any definite physicochemical variables that affect the diazotrophic activity. Nevertheless, these physicochemical drivers are expected to be involved in regulating biological parameters—heterocysts and a proportion of *A. flosaquae* biomass containing heterocysts—that were shown to be directly linked to the N_2-fixation rate in the Gulf of Riga.

Acknowledgements

We would like to express our sincerest gratitude to Lauma Buša and Māris Bērtiņš from the University of Latvia for conducting the isotope ratio mass spectrometry analysis. Further thanks go to our colleagues Alla Ivakina, Ņina Sunelika and Sintija Bušmane for nutrient analysis.

Supplementary data

Supplementary data are available at *FEMSEC* online.

Conflicts of interest statement. None declared.

Funding

This work was supported by The Latvian Council of Science (LCS) through the Fundamental and Applied Research project grant [lzp-2020/1–0063].

References

Chen X, Dolinova I, Sevcu A *et al.* Strategies adopted by Aphanizomenon flos-aquae in response to phosphorus deficiency and their role on growth. *Environ Sci Eur* 2020;**32**:1–13. DOI: 10.1186/s12302-020-00328-3.

Degerholm J, Gundersen K, Bergman B *et al.* Phosphorus-limited growth dynamics in two Baltic Sea cyanobacteria, Nodularia sp. and Aphanizomenon sp. *FEMS Microbiol Ecol* 2006;**58**:323–32.

Degerholm J, Gundersen K, Bergman B *et al.* Seasonal significance of N2 fixation in coastal and offshore waters of the northwestern Baltic Sea. *Mar Ecol Prog Ser* 2008;**360**:73–84.

Edler L. Recommendations for marine biological studies in the Baltic Sea : phytoplankton and chlorophyll. *Baltic Mar Biol* 1979;**5**:1–38.

Eigemann F, Vogts A, Voss M *et al.* Distinctive tasks of different cyanobacteria and associated bacteria in carbon as well as nitrogen fixation and cycling in a late stage Baltic Sea bloom. *PLoS One* 2019;**14**:e0223294.

Eugster O, Gruber N. A probabilistic estimate of global marine N-fixation and denitrification. *Global Biogeochem Cycles* 2012;**26**:1–15. DOI: 10.1029/2012gb004300.

Findlay DL, Hecky RE, Hendzel LL *et al.* Relationship between N2-fixation and heterocyst abundance and its relevance to the nitrogen budget of Lake 227. *Can J Fish AquatSci* 1994;**51**:2254–66.

Grasshoff K, Ehrhardt M, Kremling K. *Methods of Seawater Analysis*. Weinheim; New York: Wiley-VCH, 1999.

Hamme RC, Emerson SR the solubility of neon, nitrogen and argon in distilled water and seawater. *Deep Sea Res Part I* 2004;**51**:1517–28.

HELCOM, 2017. *Guidelines for monitoring of phytoplankton species composition, abundance and biomass*. HELCOM Monitoring Manual.

HELCOM, 2021. *Guidelines for monitoring of phytoplankton species composition, abundance and biomass*. HELCOM Monitoring Manual.

Hobbie JE, Daley RJ, Jasper S. Use of nuclepore filters for counting bacteria by fluorescence microscopy. *Appl Environ Microbiol* 1977;**33**:1225–8.

Horne AJ, Goldman CR. Nitrogen fixation in Clear Lake, California. I. Seasonal variation and the role of heterocysts. *Limnol Oceanogr* 1972;**17**:678–92.

Howarth RW, Marino R, Cole JJ. Nitrogen fixation in freshwater, estuarine, and marine ecosystems. 2. Biogeochemical controls1. *Limnol Oceanogr* 1988;**33**:688–701.

Jurgensone I, Carstensen J, Ikauniece A *et al.* Long-term Changes and Controlling Factors of Phytoplankton Community in the Gulf of Riga (Baltic Sea). *Estuaries Coasts* 2011;**34**:1205–19.

Klawonn I, Lavik G, Böning P *et al.* Simple approach for the preparation of 15-15N2-enriched water for nitrogen fixation assessments: evaluation, application and recommendations. *Front Microbiol* 2015;**6** :1–11.

Klawonn I, Nahar N, Walve J *et al.* Cell-specific nitrogen- and carbon-fixation of cyanobacteria in a temperate marine system (Baltic Sea). *Environ Microbiol* 2016;**18**:4596–609.

Kolber ZS. Getting a better picture of the Ocean's nitrogen budget. *Science* 2006;**312** :1479–80.

Konno U, Tsunogai U, Komatsu DD *et al.* Determination of total N 2 fixation rates in the ocean taking into account both the particulate and filtrate fractions. *Biogeosciences* 2010;**7**:2369–77.

Kumar K, Mella-Herrera RA, Golden JW. Cyanobacterial heterocysts. *Cold Spring Harb Perspect Biol* 2010;**2**:a000315.

Laamanen M, Kuosa H. Annual variability of biomass and heterocysts of the N -fixing cyanobacterium Aphanizomenon flos-aquae in the Baltic Sea with reference to Anabaena spp. and Nodularia spumigena. *Boreal Env Res* 2005;**10**:19–30.

Labucis A, Purina I, Labuce A *et al.* Spring seasonal pattern of primary production in the Gulf of Riga (Baltic Sea) after a mild winter. *Environ Exp Biol* 2017;**15**:247–55

Larsson U, Hajdu S, Walve J *et al.* Baltic Sea nitrogen fixation estimated from the summer increase in upper mixed layer total nitrogen. *Limnol Oceanogr* 2001;**46**:811–20.

Lindahl G, Wallstrom K. Nitrogen fixation (acetylene reduction) in Planktic Cyanobacteria in Oregrundsgrepen, SW Bothnian Sea. *Archiv Fuer Hydrobiologie AHYBAY* 1985;**104**:193–204.

Mehnert G, Leunert F, Cirés S *et al.* Competitiveness of invasive and native cyanobacteria from temperate freshwaters under various light and temperature conditions. *J Plankton Res* 2010;**32**:1009–21.

Moisander P, Lehtimäki J, Sivonen K *et al.* Comparison of 15N2 and acetylene reduction methods for the measurement of nitrogen fixation by Baltic Sea cyanobacteria. *Phycologia* 1996;**35**: 140–6.

Montoya JP, Voss M, Kahler P *et al.* A Simple, High-Precision, High-Sensitivity Tracer Assay for N(inf2) Fixation. *Appl Environ Microbiol* 1996;**62**:986–93.

Niemi Å. Blue-green algal blooms and N:P ratio in the Baltic Sea. *Acta Bot Fenn* 1979;**110**:57–61.

Olenina I, Hajdu S, Edler L *et al.* Biovolumes and size-classes of phytoplankton in the Baltic Sea. HELCOM, *Balt Sea Environ Proc* 2006;**106**:1–144.

Olofsson M, Egardt J, Singh A *et al.* Inorganic phosphorus enrichments in Baltic Sea water have large effects on growth, carbon fixation, and N2 fixation by Nodularia spumigena. *Aquat Microb Ecol* 2016;**77**:111–23.

Ploug H, Adam B, Musat N *et al.* Carbon, nitrogen and O2 fluxes associated with the cyanobacterium Nodularia spumigena in the Baltic Sea. *ISME J* 2011;**5**:1549–58.

Ploug H, Musat N, Adam B *et al.* Carbon and nitrogen fluxes associated with the cyanobacterium Aphanizomenon sp. in the Baltic Sea. *ISME J* 2010;**4**:1215–23.

Purina I, Labucis A, Barda I *et al.* Primary productivity in the Gulf of Riga (Baltic Sea) in relation to phytoplankton species and nutrient variability. *Oceanologia* 2018;**60**:544–52.

R Core Team. R: A language and environment for statistical computing. R Foundation for Statistical Computing, Vienna, Austria. 2019. https://www.R-project.org/.

Rahm L, Jönsson A, Wulff F. Nitrogen fixation in the Baltic proper : an empirical study. *J Mar Syst* 2000;**25**:239–48.

Rolff C, Almesjö L, Elmgren R. Nitrogen fixation and abundance of the diazotrophic cyanobacterium Aphanizomenon sp. in the Baltic proper. *Mar Ecol Prog Ser* 2007;**332**:107–18.

Smith VH. Low nitrogen to phosphorus ratios favor dominance by blue-green algae in lake phytoplankton. *Science* 1983;**221**:669–71.

Stal L, Walsby A. Photosynthesis and nitrogen fixation in a cyanobacterial bloom in the Baltic Sea. *Eur J Phycol* 2000;**35**:97–108.

Sveden JB, Adam B, Walve J *et al.* High cell-specific rates of nitrogen and carbon fixation by the cyanobacterium Aphanizomenon sp. at low temperatures in the Baltic Sea. *FEMS Microbiol Ecol* 2015;**91**:1–10.

Tunēns J, Aigars J, Poikāne R *et al.* Stable carbon and nitrogen isotope composition in suspended particulate matter reflects seasonal dynamics of phytoplankton assemblages in the Gulf of Riga, Baltic Sea. *Estuaries Coasts* 2022;**45**:2112–23. DOI: 10.1007/s12237-022-01071-z.

Uthermöl H. Zur vervollkommung der quantitativen phytoplankton methodik. *Mitt Int Ver Theor* 1958.

Vintila S, El-Shehawy R. Ammonium ions inhibit nitrogen fixation but do not affect heterocyst frequency in the bloom-forming cyanobacterium Nodularia spumigena strain AV1. *Microbiology* 2007;**153**:3704–12.

Voss B, Bolhuis H, Fewer DP *et al.* Insights into the physiology and ecology of the brackish-water-adapted Cyanobacterium Nodularia spumigena CCY9414 based on a genome-transcriptome analysis. *PLoS One* 2013;**8**:e60224.

Wasmund N, Voss M, Lochte K. Evidence of nitrogen fixation by non-heterocystous cyanobacteria in the Baltic Sea and re-calculation of a budget of nitrogen fixation. *Mar Ecol Prog Ser* 2001;**214**:1–14.

Wasmund N. Occurrence of cyanobacterial blooms in the baltic sea in relation to environmental conditions. *Int Revue Ges Hydrobiol Hydrogr* 1997;**82**:169–84.

White AE, Granger J, Selden C *et al.* A critical review of the 15N2 tracer method to measure diazotrophic production in pelagic ecosystems. *Limnol Oceanogr Methods* 2020;**18**:129–47.

Yoon HS, Golden JW. PatS and products of nitrogen fixation control heterocyst pattern. *J Bacteriol* 2001;**183**:2605–13.

Yurkovskis A, Kostrichkina E, Ikauniece A. *Seasonal succession and growth in the plankton communities of the Gulf of Riga in relation to long-term nutrient dynamics. Biological, Physical and Geochemical Features of Enclosed and Semi-Enclosed Marine Systems*. Springer, The Netherlands, 1999,83–94.

Zakrisson A, Larsson U. Regulation of heterocyst frequency in Baltic Sea Aphanizomenon sp. *J Plankton Res* 2014;**36**:1357–67. DOI: 10.1093/plankt/fbu055.

Zilius M, Vybernaite-Lubiene I, Vaiciute D *et al.* Spatiotemporal patterns of N2 fixation in coastal waters derived from rate measurements and remote sensing. *Biogeosciences* 2021;**18**:1857–71.